Diffusion-based Heterogeneity Models in Magnetic Resonance Imaging for Characterization of Brain Tumors: An Introductory Study

Thesis submitted to the

University of Arizona College of Medicine - Phoenix

in partial fulfillment of the requirements for the degree of

Doctor of Medicine

Christopher Goettl

Class of 2012

Mentor: John P. Karis, MD

Dedication

To my family - Thank you for your love and support.

Acknowledgments

I would like to especially acknowledge my mentor for this project, Dr. John Karis, who took the time to introduce me to the complexity of MRI and guide me through this process. Completing this paper without his teaching and vast expertise in neuroimaging would not have been possible. Thank you for all your help and support over the last several years.

Also, I want to thank Chu-Yu Lee, who acted as both colleague and teacher to me through much of this, and completed many of the critical analyses in this paper. The alpha and kurtosis maps shown were constructed using his expertise and he provided me with important data and answered countless of my questions throughout.

To Dr. Joseph Debbins, who also mentored me and took the time to teach me about the physics of diffusion MRI, thank you for your willingness to meet on many occasions and help me better understand this technology.

Finally, to Dr. Burt Feuerstein, who helped organize and oversee this process for so many of us, and who gave me personal feedback on this paper that was very helpful . Thank you for your dedication to student research.

Abstract

Recently developed diffusion-based magnetic resonance (MR) protocols have proven useful in assessing the heterogeneity of water diffusion in neural tissues, including brain tumors[1]. Based on theoretical increase in tumor cell heterogeneity compared to healthy brain[2], these emerging imaging modalities offer several potentially useful applications, such as in identifying tumor margins, establishing tumor type and grade, and for differentiating tumor recurrence from post-treatment effect. In this study an introductory subset of five patients were scanned using a multi b-value Diffusion-Weighted Image (DWI) sequence, fitted with two previously described higher-order diffusion models. The first utilized a stretched exponential model (α-DWI)[3]; the second applied a cumulant expansion model (Diffusional Kurtosis Image, DKI)[4]. These models quantified water diffusion heterogeneity using the fitted parameters α and K_{app}, respectively. The intent of this project was to gauge the potential utility of these MR models to apply diffusion heterogeneity information for characterization of brain tumors. Early results confirmed initial

hypotheses for high-grade gliomas, that (1) diffusion heterogeneity appeared greater in tumoral regions than in surrounding tissue, (2) high-grade tumors exhibited a relatively more heterogeneous diffusion pattern (lower α and higher K_{app}) compared with low-grade glioma, and (3) the metastatic tumor had unique diffusion behavior compared to the primary tumors. Overall, this introductory study generally supports the potential ability of higher-order diffusion heterogeneity models to characterize brain tumors. More detailed investigation of this application across a larger subset of patients and tumor types may be beneficial.

Table of Contents

List of Figures and Tables 8

Introduction

- Background 10
- Historical Context - Neuroimaging 11
- Imaging of Brain Tumors 13
- Diffusion MR Imaging and Higher Order Diffusion-based Heterogeneity Models 19
- Significance 35
- Aims 35

Methodology 37

Results 43

Discussion 47

Future Directions 50

Conclusion 51

References 52

List of Figures and Tables

Figures	Description	Page
Figure 1	Axial T1-weighted MR images of pilocytic astrocytoma, with and without contrast.	16
Figure 2	MR spectroscopy data for a patient with oligoastrocytoma	18
Figure 3	Equation used to construct diffusion weighted images (DWI)	21
Figure 4	Glioblastoma in the right temporal lobe, with DWI image (figure 4c)	23
Figure 5	T1-weighted MR and ADC map of patient with left temporal lobe glioblastoma	25
Figure 6	(A) Contrast-enhanced T1-weighted image (A), T2-weighted image (B), and Diffusion Tensor Imaging directional color map (C) of a patient with ganglioma located in the thalamus	27

Figure 7	Two histograms for conceptual representation of homogeneous and heterogeneous water diffusion behavior	29
Figure 8	The stretched exponential model used to construct α heterogeneity maps	32
Figure 9	Cumulant expansion model used in Diffusional Kurtosis Imaging (DKI)	34
Figure 10	Imaging maps constructed for five patients	39
Figure 11	Tumoral area for patient (b), defined by area of increased signal on T2-weighted image	41

Tables	**Description**	**Page**
Table 1	Values for imaging parameters α and K_{app}, as well as apparent diffusion coefficient (ADC) for selected regions of interest in patients studied	44

Introduction

Background

Brain and other nervous system tumors account for approximately 1.4 percent of new primary cancer cases in the United States[5]. Even more common within the brain are metastatic tumors from other primary sites, which have been estimated to affect 20 to 40% of all adult cancer patients, or 150,000 to 170,000 persons per year[6]. Worldwide, hundreds of thousands more are affected annually[7]. Although brain tumors occur less frequently than tumors of more common primary sites, such as the breast, prostate, lung, and colon, they are often refractory to all available treatment, are more difficult to manage surgically, and confer extremely high morbidity and mortality to patients.

Clinical management of brain tumor patients has increasingly relied on neuroimaging, in particular MR imaging, to provide information central to patient care. Contributions of MR to clinical management include accurate initial diagnosis, tumor localization, surgical planning, monitoring response to treatment, and determining prognosis, among others. While neuropathologic analysis of tumor

tissue remains the most definitive diagnostic tool, MR offers a broad variety of methods that can be used to characterize and grade brain tumors non-invasively.

One sub-category of MR imaging, diffusion-based MR, has developed considerably over the last decade[8]. Diffusion-based MR imaging fundamentally describes molecular water mobility within tissue – which can be correlated with specific anatomy and pathology. Within this category, more complex diffusion-based models have been recently described that focus on heterogeneity of water movement[9 10]. These models may be applicable particularly in the diagnosis and management of brain tumors[11 12].

Due to disease incidence, relatively grave morbidity and mortality, and the central role of imaging in patient management of intracerebral neoplasms, the potential upside of novel MR modalities to further characterize tumors is significant. The value of such modalities are only likely to increase in the future, particularly as treatment options become more effective and targeted.

Historical Context - Neuroimaging

Innovation in neuroimaging has accelerated remarkably over the past

century, starting with Röntgen's discovery of the X-ray for human imaging in 1895. In 1918, Dr. Charles Dandy first described injection of air into the lateral ventricles for the diagnosis of tumors and hydrocephalus[13], and shortly after in 1919 he pioneered the pneumoencephalogram to describe morphology of the cerebral cortex[14]. In 1927, neurologist Egas Moniz of Portugal pioneered the use of iodinated contrast through the carotid arteries, enabling the initial *in vivo* visualization of the cerebral vasculature[15].

After decades of mostly incremental improvements, the early 1970s produced a remarkable leap forward with the advent of computed tomography (CT) by Sir Godfrey Houndsfield in England. For the first time, brain anatomy could be directly imaged in a non-invasive manner, allowing visualization of almost any brain pathology in previously unseen detail[16]. Thus, the emergence of CT gave birth to a new era in neuroimaging.

Shortly thereafter, during the late 1970s and early 1980s, another novel technology emerged. Magnetic resonance imaging was developed, utilizing a powerful magnetic field and pulses of radiofrequency energy to create detailed images of human tissues. Advantages of MR - including relatively high contrast resolution, the

ability to produce images in any three-dimensional plane, and lack of ionizing radiation exposure - led to widespread research and rapid adoption into clinical imaging over the following decades.

Neuroimaging of Brain Tumors

Contemporary imaging of brain tumors falls almost entirely on the shoulders of CT and MR, owing chiefly to these modalities' superior ability to display brain anatomy over alternative imaging methods. The diagnostician uses the gross anatomic rendering in combination with patient information such as age, sex, risk factors, and tumor morphology, to arrive at a diagnosis. Additional information such as blood-brain barrier behavior or tissue chemical composition can be gleaned and may aid in the diagnosis.

CT imaging relies on the same physical principles as basic radiographs, transmitting ionizing radiation (X-rays) through patient tissue to an image detector on the opposite side. Differences in atomic density within tissues produces varying degrees of attenuation of the beam, which determines the energy measured by the detector for image creation. Unlike radiographs, however, CT data is gathered by spinning the transducer around the patient to create a 3-dimensional

data set. Innovations such as multi-detector CT (MDCT) scanners and three-dimensional computer reconstruction of images, as well as the decreased cost of CT studies relative to MR, have contributed to widespread use of CT as an initial diagnostic exam for brain pathology. However the presence of biologically significant levels of ionizing radiation often limits the number of CT exams that are medically acceptable for a particular patient.

MR imaging does not make use of ionizing radiation such as X-rays. Instead, MR uses a powerful magnetic field (with field strength of 3 Tesla or greater in modern scanners) to align protons along a magnetic vector. Then, a specially calibrated radiofrequency (RF) pulse is directed into the subject. The RF pulse momentarily excites the protons into a higher-energy state, and shortly thereafter the protons return back to their initial energy state, releasing back some of the energy they absorbed. The amount of energy released by anatomic tissue is different depending on its physical characteristics. A sensor measures this released energy, and that data is used to construct the MR image. Advantages of MR over CT include the previously mentioned absence of radiation, and better contrast resolution for soft-tissue imaging. However, total cost for an MR study typically exceeds

that of CT, often acting as a barrier to use.

Intravenous contrast agents are commonly used in both CT and MR studies to expand the breadth of imaging information that can be collected. In CT, contrast agents with relatively high atomic numbers compared to anatomic tissue are used (such as iodine-based contrast), in order to make use of CT's ability to differentiate based on density. This can be particularly useful in studies in which vascular information about a tissue or vessel is needed. In MR, agents with paramagnetic properties (such as gadolinium) are used intravenously in order to respond to MR's use of magnetism. Practically, these agents provide additional useful information by differentiating anatomy based on arterial and venous filling patterns, differences in blood-brain barrier properties, and by highlighting vasculature. Figure 1 shows a MR of the head both with and without intravenous gadolinium[17].

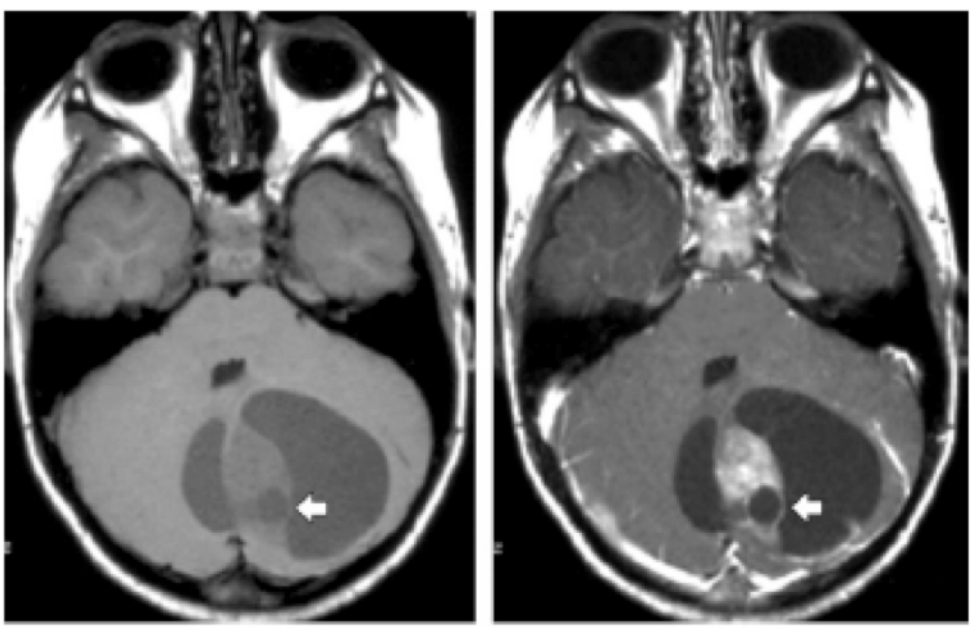

Figure 1: Pilocytic astrocytoma. (a) Axial nonenhanced T1-weighted MR image shows a cerebellar mass surrounded by a fluid-filled cyst. (b) Axial contrast-enhanced T1-weighted MR image shows intense enhancement of the tumor, but the rim surrounding cystic fluid does not enhance. Cystic mass with a mural nodule in the cerebellum is classic for a pilocytic astrocytoma.

Other specialized methods, such as MR spectroscopy, provide information about chemical properties within a defined tissue, rather than special anatomic information. Figure 2 shows a depiction of MR spectroscopy and its quantification of the chemical composition of brain tissue[18].

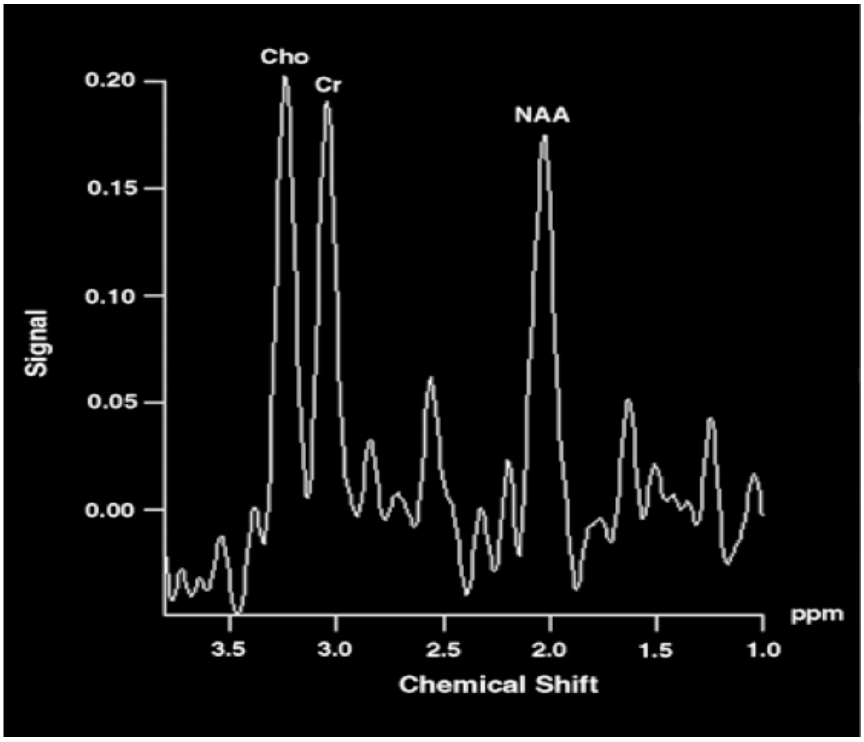

Figure 2: MR spectroscopy data for a patient with oligoastrocytoma. Data indicate mild elevation of choline (Cho) compared with creatine (Cr). NAA = *N*-acetyl aspartate

Contrast-enhancement and MR spectroscopy are examples of using vascular or chemical properties of tissues to differentiate anatomy and pathology. However, these are certainly not the only possible methods available for differentiating tissue, and in some scenarios not sufficient for making a definitive diagnosis. For this reason, new ways of characterizing and differentiating anatomy *in situ* are the focus of ongoing innovation in imaging research, particularly in MR.

One recently suggested MR model that will be the focus of this paper attempts to use diffusion properties of water within human tissues in order to create new and useful images to describe brain tumors.

Diffusion MR Imaging and Higher Order Diffusion-based Heterogeneity Models

Diffusion MR imaging generally encompasses modalities that offer information regarding the diffusion characteristics of water within tissues. Diffusion-based MR encompasses a spectrum of modalities, from the more basic Diffusion-Weighted Imaging (DWI) to higher-order modalities that provide more specific diffusion

information.

Fundamentally, DWI uses MR properties of protons to provide information about water diffusion within a specified region of anatomy. The central concept relies on the fact that various neuropathology can alter "normal" diffusion characteristics, potentially relating to differences in cell membrane functionality or intracellular contents. This imaging technique has been clinically applied in neurology to early detection of ischemic stroke[19], assessment of neural tissue viability[20], and in assessment of brain tumors[21].

Technically, DWI uses two magnetic pulse gradients to de-phase, and then re-phase protons. Protons existing in environments with more Brownian motion (e.g., more diffusion) will not re-phase as uniformly, ultimately giving off less MR signal. Conversely, protons in low-diffusion environments will re-phase to a greater extent, and produce greater signal. The amount of signal can be mathematically related to the amount of diffusion by the equation shown in figure 3. Restricted diffusion, as often seen in ischemic stroke, is bright on DWI.

$$\frac{S}{S_0} = e^{-\gamma^2 G^2 \delta^2 (\Delta - \delta/3) D} = e^{-bD}$$

Figure 3: Equation used to create Diffusion-Weighted Images, where S_0 is the signal intensity without the diffusion weighting, S is the signal with the gradient, γ is the gyromagnetic ratio, G is the strength of the gradient pulse, δ is the duration of the pulse, Δ is the time between the two pulses, and finally, D is the diffusion-coefficient.

In DWI models, diffusion information is typically gathered for three gradient directions (corresponding to x, y, and z planes) via three imaging acquisitions, and then averaged to produce the mean water diffusion distance within a particular imaging voxel. DWI maps show restricted average diffusion as bright, while normal or increased diffusion is darker. Figure 4(c) shows a DWI map of a glioblastoma.

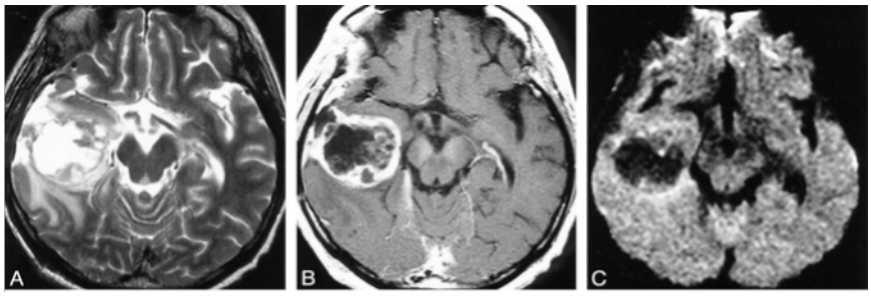

Figure 4: Glioblastoma in the right temporal lobe.
(A) T2-weighted image showing tumor of mixed intensity with surrounding edema. (B) T1-weighted image showing heterogeneous enhancement after intravenous injection of contrast medium. (C) On DWI, a solid portion of the tumor is isointense to moderately high in intensity, typical of high-grade glioma. Edema surrounding the tumor is isointense.

One potential pitfall related to DWI methodology is a phenomenon known as "T2 shine through," a mechanism that can cause increased signal on DWI, but not directly as a result of diffusion changes. This is due to the mathematical model on which DWI is founded, which implies that DWI signal includes T2 signal as part of the total signal measured for imaging. In order to eliminate T2 shine-through, the mathematical model is manipulated to solve for the diffusion co-efficient (represented by D in figure 3).

In order to address the sensitivity of DWI to effects of underlying T2 contrast, another similar modality has been proposed that uses the diffusion co-efficient as the sole basis for image contrast. In this model, multiple *b* values are used to solve for the diffusion co-efficient *D* at a given anatomic location. The diffusion co-efficient is technically described as the apparent diffusion co-efficient (ADC), due to the fact that water movement is not actually unrestricted in live tissue. In fact, measured diffusion is influenced by additional factors *in situ*, such as blood flow through microvasculature and diffusion restriction resulting from cellular compartments. ADC maps show reduced diffusion as dark, and increased diffusion as bright, as seen in figure 5[22].

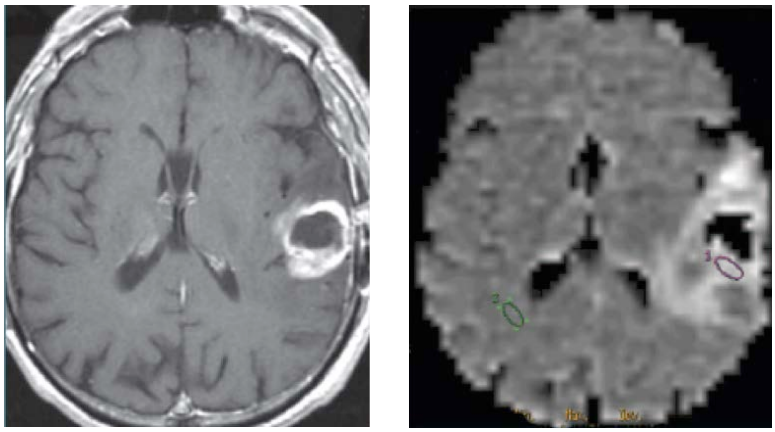

Figure 5: At left, axial T1-weighted MR with gadolinium shows a partially resected left temporal lobe glioblastoma with rim enhancement. At right, axial ADC map in the same patient showing increased mean diffusion (ADC value was 183% when compared to contralateral normal brain).

DWI and ADC maps provide insight into average diffusion within a defined imaging space. In order to gain insight into more detailed diffusion information (for example, the *directional* diffusion of water in a tissue), more specific diffusion-based modalities are used. Diffusion tensor imaging (DTI) is another diffusion-based MR protocol that expands data acquisition to six or more gradient directions. This allows directional mapping of water diffusion in tissues such as nerve axons, where water may be able to easily diffuse along cellular tracts, but not as easily across cell membranes. Figure 6 shows an example of a DTI map with color-coded directional diffusion of water along axonal tracts within the brain[23].

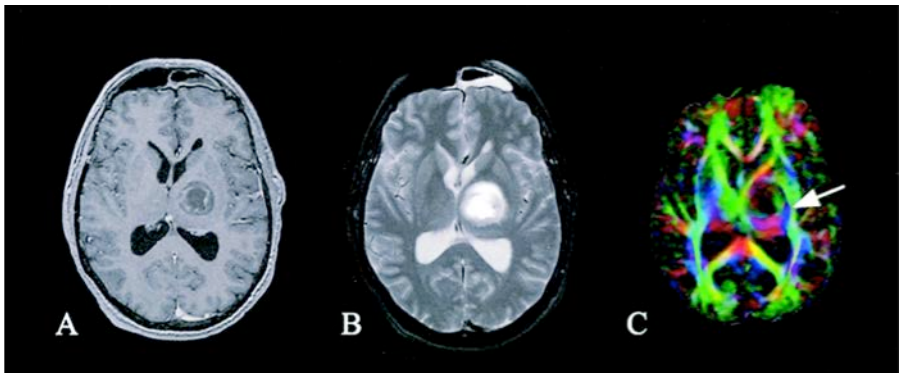

Figure 6: (A) Contrast-enhanced T1-weighted image (A), T2-weighted image (B), and Diffusion Tensor Imaging directional color map (C) of a patient with ganglioma located in the thalamus. The DTI color map shows directional diffusion gradients along axonal tracts.

Whereas DTI imaging is able to add information about *directional* water diffusion[24], other diffusion-based protocols exist that can provide information about the *heterogeneity* of water diffusion. The concept of heterogeneity applied to water movement implies a greater degree of variability in distance and direction of molecular diffusion. Schematic histograms of homogeneous versus heterogeneous water diffusion patterns are shown in figure 7.

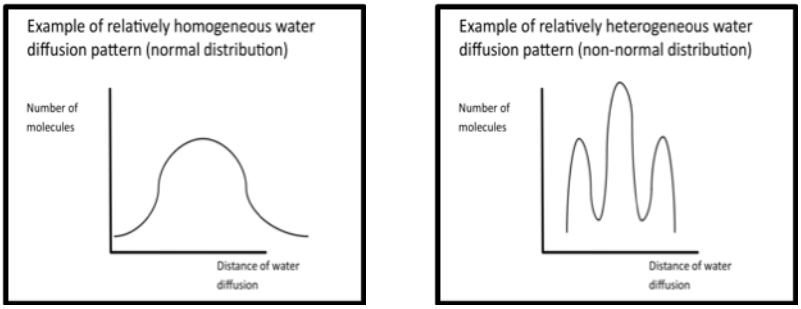

Figure 7: Two histograms for conceptual representation of water diffusion behavior. At left, generally homogeneous, or "Gaussian" diffusion. At right, generally heterogeneous, or "non-Gaussian" diffusion.

Diffusion heterogeneity models examine how uniform water diffusion properties are within a defined space. This imaging methodology is theoretically based on known characteristics of tumors themselves; in particular, the fact that tumor cells tend to be more heterogeneous in size and function when compared to healthy tissue[25]. Because high-grade gliomas have been postulated to be generally more heterogeneous than low-grade tumors pathologically, this presents a potential opportunity to use these heterogeneity-based imaging studies to gain insight into tumor grade.

Two models used to quantify diffusion heterogeneity in this particular work are a recently described stretched exponential model (α-DWI)[26 27] and also a cumulant expansion model (DKI)[28 29]. These modalities attempt to quantify diffusion heterogeneity using the parameters α and K_{app}, respectively. Whereas DWI assumes a generally uniform water diffusion behavior within any imaging voxel, these higher-order modalities do not.

The first model, the α-DWI model, provides a diffusion heterogeneity index, varying between 0 and 1. An α value of 0 indicates stronger multi-exponential signal decay (more heterogeneous diffusion behavior), while an α value of 1 indicates a mono-exponential decay

(more homogeneous diffusion behavior). This model is described in figure 8.

$$S(b)/S_o = \exp(-(b \times DDC)^{\alpha})$$

Figure 8: Stretched-exponential model, where *S(b)* is the signal magnitude with diffusion weighting *b*, and *So* is the signal magnitude with no diffusion weighting. α represents the diffusion heterogeneity parameter

DKI represents the second higher-order diffusion heterogeneity model examined in this work, representing a clinically relevant extension of previously described diffusion tensor imaging[30]. Generally, it quantifies water diffusion's departure from a "normal," or Gaussian, distribution[31]. A kurtosis co-efficient of 0 would represent more Gaussian distribution of water diffusion distances (more homogeneous diffusion), while a value of 1 would represent complete departure from normal distribution (heterogeneous diffusion behavior). In other words, the kurtosis parameter is a marker of non-Gaussianity of water diffusion. Pathophysiologically, non-Gaussian diffusion behavior is thought to result from properties of tissue microstructure that result in diffusion barriers or compartments, altering normal molecular movement patterns[32]. This imaging modality uses a cumulant expansion model, shown in figure 9[33].

$$\ln[S(b)] \approx \ln(S_0) - bD(t) + \frac{1}{6}[bD(t)]^2 K(t)$$

Figure 9: Cumulant expansion model used in Diffusional Kurtosis Imaging (DKI). S(b) is the signal with diffusion weighting, S(o) without diffusion weighting, the b value (in s/mm^2) is a function of diffusion gradient strength, D is the diffusion co-efficient, and K the apparent kurtosis co-efficient

Significance

Higher-order diffusion-based heterogeneity models could be significant in the diagnosis and management of brain tumors in several ways. First, these modalities could help categorize and grade tumors based on their characteristic diffusion indices. This could provide clinical benefit by improving diagnostic yield of brain biopsies, and could one day even serve as a suitable non-invasive alternative to invasive diagnostic methods in some cases. Second, heterogeneity markers could be used to differentiate tumor from surrounding brain, thus helping to define tumor margins pre-operatively. When used in conjunction with conventional contrast-enhanced T1 images, this could improve surgical outcomes by maximizing preservation of healthy brain area after resection. Third, these imaging models could be applied to help differentiate post-treatment effect from recurrent tumor. Patients treated with external beam radiation therapy (EBRT) and/or chemotherapeutic agents could be more accurately monitored for tumor recurrence and treated accordingly.

Aims

The aims of this study will be (1) to initially assess the potential

of the above heterogeneity models for the purposes of tumor grading, and (2) to consider an alternative method for differentiating tumor areas from surrounding brain parenchyma.

A subsequent study is ongoing to examine the utility of these models for differentiating post-treatment effect from tumor recurrence, but will not be addressed in this work.

Methodology

To initiate this introductory study, five patients were scanned with full institutional review board approval at a major metropolitan medical center. All were undergoing clinical contrast-enhanced stereotactic MRI for previously diagnosed tumor evaluation. Each tumor was pathologically identified and graded at time of surgery, using World Health Organization (WHO) classification system. One patient had metastatic disease (a), one had a low-grade glioma (WHO grade II), and three had high-grade gliomas (WHO grade III or IV).

Research sequences were added to existing clinical scans with patient approval. Echo planar imaging (EPI) sequences were implemented on a General Electric 3T scanner using 40mT/m gradients. DWI images were acquired using three gradient directions along the X, Y and Z axes and using six b-values (0, 500, 1000, 1500, 2000, and 2,500 s/mm^2). Imaging parameters used were TR/TE = 4000/104 ms, NEX = 6, slice thickness 5mm, FOV 240x240 mm^2, and matrix 128x128.

Two discrete regions were identified for further analysis in each patient. Tumor area was defined using standard gadolinium-enhanced

T1-weighted MR. Peri-tumoral areas were identified by abnormal T2-weighted signal around the tumor, signifying surrounding edema. These regions are shown in figure 10, along with constructed maps for previously described parameters α and K_{app}.

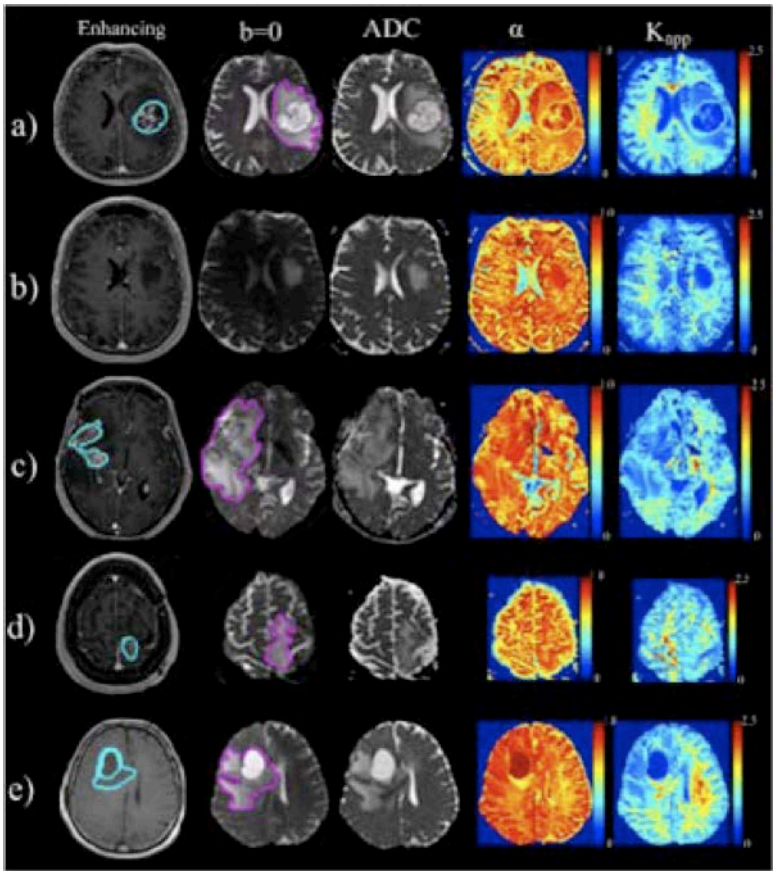

Figure 10. Patients (a) through (e), with tumoral regions defined by the area of enhancement on T1 imaging (blue outline) and peri-tumor regions defined using area of increased T2-weighted signal surrounding the tumor (purple). For patient (b), only a tumoral region was identified (see figure 11).

Patient (b) with low-grade glioma had no area of well-defined surrounding edema on T2 images, so this region of interest (ROI) was excluded from the analysis. Tumor ROI for patient (b) was defined using T2 b=0 image, shown in figure 11.

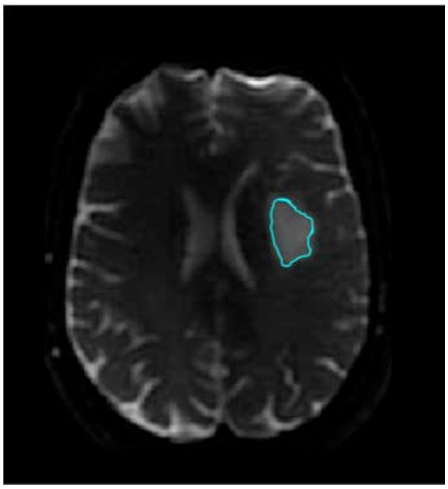

Figure 11. Tumoral area for patient (b), defined by area of increased signal on T2-weighted image (b=0). No distinct area of peri-tumoral edema was identified, so this ROI was excluded

Stretched exponential and second-order cumulant expansion models were fitted to the data using the Levenberg-Marquardt algorithm in MATLAB (Mathworks, Inc.) Unique α and K_{app} values were recorded for each region of interest described above. Data below the noise floor were excluded from the data fitting.

After constructing diffusion maps (Figure 10, right two columns) using these heterogeneity parameters, a clinical neuroradiologist with over 25 years of experience reviewed the images and generally compared tumor margins to those visible on the conventional T1 and T2-weighted images.

Results

Data from each defined ROI for each patient are shown in Table 1.

Type	Metastasis		Low-grade glioma		High-grade glioma					
Case	A		B		C		D		E	
ROI	Tumor	Peri	Tumor	Peri	Tumor	Peri	Tumor	Peri	Tumor	Peri
ADC	2.90± 0.50	1.80± 0.40	1.90± 0.17		1.70± 0.70	2.00± 0.20	1.50± 0.15	1.7± 0.46	1.20± 0.34	1.70± 0.35
α	0.78± 0.12	0.77± 0.05	0.87± 0.04	-	0.76± 0.08	0.80± 0.03	0.76± 0.04	0.77± 0.04	0.73± 0.08	0.79± 0.04
K_{app}	0.36± 0.15	0.58± 0.14	0.36± 0.07	-	0.55± 0.14	0.46± 0.07	0.60± 0.06	0.55± 0.07	0.84± 0.24	0.55± 0.17

Table 1: Values of fitted parameters α and K_{app} of tumoral and peritumoral regions for five patients with brain tumors. Patient B had no clearly defined area of surrounding edema, so data was not listed for this region of interest. ADC values are (10^{-3} mm^2/s), while α and K_{app} are unitless metrics.

In the high-grade gliomas (c – e), tumor areas showed generally more heterogeneity than in surrounding brain (lower α and higher $K_{app)}$, indicating more erratic diffusion behavior in the tumor than in assumed healthy brain. However, these results were not significant when margin of error was taken into account. ADC was generally lower in high-grade primary tumor regions than corresponding peri-tumor regions, indicating lower relative diffusion. This data is consistent with prior studies that have shown higher ADC values in low-grade astrocytomas compared to glioblastomas[34], implying a negative correlation between tumor grade and average diffusion.

When compared to the low-grade glioma (b), tumor areas in high-grade gliomas did appear to behave differently; high-grade tumors displayed more heterogeneous diffusion parameters (noted by lower α and higher K_{app}) when compared with the low-grade case.

The metastatic case (a) behaved differently, with less diffusion heterogeneity in the tumoral area than in surrounding brain. The metastasis had tumoral α values similar to that of high-grade gliomas, but K_{app} values corresponding to the low-grade case. ADC in the metastasis was much higher than surrounding brain, possibly due to altered cellularity.

In addition, we found that there exists a mismatch among the regions of heterogeneity by α and K_{app} maps and T1-weighted enhancing regions, potentially suggesting a novel approach to assessing tumor border.

Discussion

The sample size used in this work was quite small, and only sufficient to generally suggest the potential of these heterogeneity-based methods for characterizing brain tumors. However, early data suggest some promising potential in tumor grading, and possibly as an alternative method of defining tumor boundaries.

With respect to tumor margins, there may be subtle but real differences in defining tumor morphology by conventional contrast-enhanced studies and these heterogeneity models. This reflects a different underlying mechanism, in that contrast-enhanced imaging differentiates tumor from normal tissue based on blood-brain barrier properties as opposed to the water diffusion properties discussed here. Better identification of tumor margins could provide value by improving diagnostic yield of tissue biopsies.

This application could be especially beneficial in treatment centers utilizing a high number of biopsies for patient care. However, this becomes less important in many centers where tumor debulking and adjuvant therapy is the norm and biopsy is rarely used. In these centers, differentiating post-treatment effect from recurrence becomes

more critical – another potential use of these imaging parameters that could be developed further. In surgical planning where excision occurs near areas of eloquent brain versus less-eloquent brain, minimizing the amount of healthy tissue removed becomes increasingly important.

As for tumor grading, our early data indicated that high-grade gliomas had reduced overall diffusion (lower ADC) compared with lower-grade gliomas, but that the diffusion was more heterogeneous in nature (shown by α and K_{app}). This likely reflects increased overall cellularity of these tumors, decreased extracellular space, and more disorganized intracellular architecture and membrane transport properties. ADC values have previously been shown to correlate negatively with degree of cellularity in brain tumors[35], which seems to be confirmed again here. Accordingly, the low-grade case had diffusion indicators much closer to that of healthy tissue, indicating only modest changes in cellularity and water diffusion behavior.

The aforementioned grading applications are perhaps the most promising areas for these emerging diffusion-based models. As chemotherapeutic, radiation, and surgical treatment options become more specific to tumor type and grade, this type of classification is critical. Keeping in mind that MR provides a non-invasive option

compared to invasive diagnostic approaches such as biopsy, these recently developed heterogeneity models could become valuable tools in diagnosis and ongoing management of astrocytic tumors.

Future Directions

Larger patient sets with distinct tumor histology (e.g., low-grade glioma, high-grade glioma, meningioma, medulloblastoma, and metastatic disease from various primary sites) could be examined in more detail. These parameters could be explored for diagnosis of other solid organ tumors, such as liver, colon, breast, or bone cancer. Additionally, it would be interesting to correlate these imaging parameters with different histopathologic characteristics, such as necrosis, inflammation, hemorrhage, and cell density.

Following this study, additional analysis is underway to further assess the applicability of these diffusion-based models to differentiate post-treatment change from tumor recurrence.

Conclusions

This exercise shows the potential utility of diffusion-based heterogeneity parameters α and K_{app} to gain further insight into tumor pathology. Specifically, these techniques may prove promising diagnostically in determining tumor type and grade, especially in differentiating high-grade gliomas from lower-grade gliomas. This differentiation may become increasingly valuable as treatment options improve in coming decades. With respect to tumor margins, these modalities may prove a useful alternative to conventional methods of defining boundaries. Especially in biopsy-heavy centers, potential exists to improve diagnostic yield of brain biopsy. Application of these models to differentiate tumor recurrence from post-treatment change is ongoing. This exercise is consistent with other recent works in demonstrating the utility of parameters α and K_{app} in understanding brain anatomy and pathology [36] [37] [38] [39].

References

[1] Kwee T, Galban C, Ivancevic M, et al. Intravoxel water diffusion heterogeneity of human high-grade gliomas. *NMR Biomed*. 2010;23(2):179-87.

[2] Inda MM, Bonavia R, Mukasa A, et al. Tumor heterogeneity is an active process maintained by a mutant EGFR-induced cytokine circuit in glioblastoma. *Genes Dev*. 2010;15(16):1731-45.

[3] Bennett KM, Schamainda KM, Bennett RT, Rowe DB, Lu H, Hyde JS. Characterization of continuously distributed cortical water diffusion rates with a stretched-exponential model. *Magn Reson Med*. 2003;50(4):727-34.

[4] Jensen JH, Helpern JA, Ramani A, Lu H, Kaczynski K. Diffusional kurtosis imaging: the quantification of non-gaussian water diffusion by means of magnetic resonance imaging. *Magn Reson Med*. 2005;53(6):1432-40.

[5] American Cancer Society. Cancer Facts & Figures 2011. http://www.cancer.org/Research/CancerFactsFigures/CancerFactsFigures/cancer-facts-figures-2011. Accessed November 10, 2011.

[6] Newton HB, Jolesz FA. *Handbook of Neuro-Oncology NeuroImaging*. 1st ed. New York, NY: Elsevier; 2008:1.

[7] Ferlay J, Shin HR, Bray F, Forman D, Mathers C and Parkin DM. GLOBOCAN 2008 v1.2, Cancer Incidence and Mortality Worldwide: IARC CancerBase No. 10 [Internet]. Lyon, France: International Agency for Research on Cancer; 2010. Available from: http://globocan.iarc.fr, accessed on October 12, 2011.

[8] Maier SE, Sun Y, Mulkern RV. Diffusion imaging of brain tumors. *NMR Biomed*. 2010;23(7):849-64.

[9] Lu H, Jensen JH, Ramani A, Jalpern JA. Three-dimensional characterization of non-gaussian water diffusion in humans using diffusion kurtosis imaging. *NMR Biomed.* 2006;19(2):236-47.

[10] Bennett KM, Hyde JS, Schmainda KM. Water diffusion heterogeneity index in the human brain is insensitive to the orientation of applied magnetic field gradients. *Magn Reson Med*. 2006;56(2):235-9.

[11] Kwee TC, Galban CJ, Tsien C, et al. Intravoxel water diffusion heterogeneity imaging of human high-grade gliomas. *NMR Biomed*. 2010;23(2):179-87.

[12] Raab P, Hattingen E, Franz K, Zanella FE, Lanfermann H. Cerebral gliomas: diffusional kurtosis imaging analysis of microstructural differences. *Radiology*. 2010;254(3):876-81.

[13] Dandy WE. Ventriculography following the injection of air in to the cerebral ventricles. *Ann Surg*. 1918; 68(1): 5–11.

[14] Dandy WE. Roentgenography of the brain after the injection of air into the spinal canal. *Ann Surg* 1919; 70:397.

[15] Moniz EL. L'Angiographie cerebrale. *Masson & Cie*. 1934;142–214.

[16] Leeds N, Kieffer S. Evolution of Diagnostic Neuroradiology from 1904 to 1999. *Radiology*. 2000;217, 309-318.

[17] Smirniotopoulos JG, Murphy FM, Rushing EJ, Rees JH, Shroeder LT. Patterns of Contrast Enhancement in the Brain and Meninges. *Radiographics* 2007; 27:525–551.

[18] Spampinato MV, Smith JK, Kwock L, et al. Cerebral blood volume measurements and proton MR spectroscopy in grading of oligodendroglial tumors. *AJR Am J Roentgenol*. 2007;188(1):204-12.

[19] Mullins ME, Schaefer PW, Sorensen AG, et al. CT and conventional and diffusion-weighted MR imaging in acute stroke: study in 691

patients at presentation to the emergency department. *Radiology* 2002;224(2):353-60.

[20] Schaefer PW, Ozsunar Y, He J, et al. Assessing tissue viability with MR diffusion and perfusion imaging. *AJNR Am J Neuroradiol*. 2003;24(3):436-43.

[21] Kono K, Inoue Y, Nakayama K, et al. The role of diffusion-weighted imaging in patients with brain tumors. *AJNR Am J Neuroradiol*. 2001;22(6):1081-8.

[22] Diffusion-weighted and Perfusion MR Imaging for Brain Tumor Characterization and Assessment of Treatment Response. Provenzale JM, Srinivasan M, Barboriak DP. *Radiology*. 2006;239:632-649.

[23] Laundre BJ, Jellison BJ, Badie B, Alexander AL, Field AS. Diffusion Tensor Imaging of the Corticospinal Tract before and after Mass Resection as Correlated with Clinical Motor Findings: Preliminary Data. *AJNR Am J Neuroradiol* 2005;26:791–796.

[24] Nucifora PG, Verma R, Lee SK, Melhem ER. Diffusion-tensor MR imaging and tractography: exploring brain microstructure and connectivity. *Radiology*. 2007;245(2):367-84.

[25] Inda MM, et al. (2010)

[26] Bennett KM, Schmainda KM, Bennet RT, Rowe DB, Lu H, Hyde JS. Characterization of continuously distributed cortical water diffusion rates with a stretched-exponential model. *Magn Reson Med*. 2003;50(4):727-34.

[27] Kwee TC, Galban CJ, Tsien C, et al. Intravoxel water diffusion heterogeneity imaging of human high-grade gliomas. *NMR Biomed*. 2010;23(2):179-87.

[28] Jensen JH, Helpern JA, Ramani A, Lu H, Kaczynski K. Diffusional kurtosis imaging: the quantification of non-gaussian water diffusion by

means of magnetic resonance imaging. *Magn Reson Med*. 2005;53(6):1432-40.

[29] Jensen JH, Helpern JA. MRI quantification of non-Gaussian water diffusion by kurtosis analysis. *NMR Biomed*. 2010;23(7):698-710.

[30] Fieremans E, Jensen JH, Helpern JA. White matter characterization with diffusional kurtosis imaging. *Neuroimage*. 2011 Sep 1;58(1):177-88.

[31] Lu H, Jensen JH, Ramani A, Jalpern JA. Three-dimensional characterization of non-gaussian water diffusion in humans using diffusion kurtosis imaging. *NMR Biomed*. 2006;19(2):236-47.

[32] Jensen JH, Helpern JA. MRI quantification of non-Gaussian water diffusion by kurtosis analysis. *NMR Biomed*. 2010;23(7):698-710. *NMR Biomed*. 2010 Aug;23(7):698-710.

[33] Jensen JH, et al. (2010)

[34] Kono K, Inoue Y, Nakayama K, et al. The role of diffusion-weighted imaging in patients with brain tumors. *Am J Neuroradiol*. 2001; 22:1081–1088.

[35] Yamashita Y, Kumabe T, Higano S, Watanabe M, Tominaga T. Minimum apparent diffusion coefficient is significantly correlated with cellularity in medulloblastomas. *Neurol Res*. 2009;31(9):940-6.

[36] Raab P, Hattingen E, Franz K, Zanella FE, Lanfermann H. Cerebral gliomas: diffusional kurtosis imaging analysis of microstructural differences. *Radiology*. 2010 Mar;254(3):876-81.

[37] Wu EX, Cheung MM. MR diffusion kurtosis imaging for neural tissue characterization. *NMR Biomed*. 2010;23(7):836-48.

[38] Kwee TC, Galban CJ, Tsien C, et al. Intravoxel water diffusion heterogeneity imaging of human high-grade gliomas. *NMR Biomed*. 2010;23(2):179-87.

[39] Cheung MM, Hui ES, Chan KC, Helpern JA, Qi L, Wu EX. Does diffusion kurtosis imaging lead to better neural tissue characterization? A rodent brain maturation study. *Neuroimage.* 2009 Apr 1;45(2):386-92.